

A Multek White Paper  
March 2017

## Characterizing Lossy PCB Interconnects Using a TDR Instrument



**MULTEK**

One-stop Interconnect Solutions Provider



Executive Summary .....	3
Interconnect Impedance in the Time Domain .....	4
NEXT Ratios in Greater Detail .....	8
Impact of Interconnect Losses on Measured Impedance .....	10
The importance of Slope in Characterizing Lossy Interconnects .....	12
Conclusions. ....	13

## **EXECUTIVE SUMMARY**

Extracting the characteristic impedance of a low loss PCB interconnect using a TDR (Time Domain Reflectometer) instrument is relatively easy to accomplish because the impedance curve as a function of distance along the interconnect remains relatively constant.

But if the PCB interconnect is lossy, then the characteristic impedance curve will have a rising slope. This rising slope can make compliance with non-rising (horizontal) limits difficult, and in extreme cases impossible – even though the interconnect meets the design specifications.

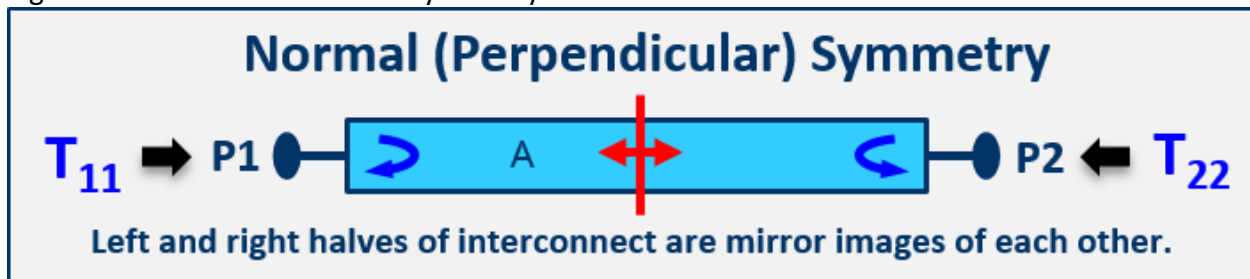
This white paper explores the basis for this rising slope and proposes an alternative to the traditional horizontal limit lines that more accurately quantifies the impedance properties of the interconnect.

## Interconnect Impedance in the Time Domain

A TDR (Time Domain Reflect) instrument can measure the amplitude and shape of a pulse injected into a PCB interconnect (the outbound signal) and the amplitude and shape of any responses that are reflected back toward the TDR (the reflected signal). The reflected signal can then be divided by the outbound signal to obtain a T-parameter REFL (reflection) ratio.<sup>1</sup>

For a single-ended (one trace) interconnect, two T-parameter ratio measurements can be made: the  $T_{11}$  ratio corresponds to the case where the TDR is connected to the “left” P1 interconnect port and the  $T_{22}$  ratio corresponds to the case where the TDR is connected to the “right” P2 port.<sup>2</sup>

Figure 1: Definition of Normal Symmetry



Referring to Figure 1, if the interconnect is symmetrical about the center of the interconnect, then the left and right halves of the interconnect are mirror images of each other and  $T_{11} = T_{22}$ .

T-parameter REFL ratios can be converted into an equivalent “impedance looking into the port” provided the source impedance of the TDR is known. For most cases, the TDR source impedance is  $50\ \Omega$ , in which case the impedance looking into ports P1 and P2 can be computed using the following two formulas:

$$Z_{11} = 50 \cdot \frac{1+T_{11}}{1-T_{11}}, \quad Z_{22} = 50 \cdot \frac{1+T_{22}}{1-T_{22}} \quad (1)$$

These formulas for converting the two  $T_{xx}$  values into their corresponding  $Z_{xx}$  values, are non-linear.  $T_{xx} = 0$  corresponds to  $Z_{xx} = 50\ \Omega$ ,  $T_{xx} = 1$  corresponds to  $Z_{xx} = \infty\ \Omega$ , while  $T_{xx} = -1$  corresponds to  $Z_{xx} = 0\ \Omega$ . Positive values correspond to impedances greater than the TDR source impedance, while negative values correspond to impedances less than the TDR source impedance.<sup>3</sup>

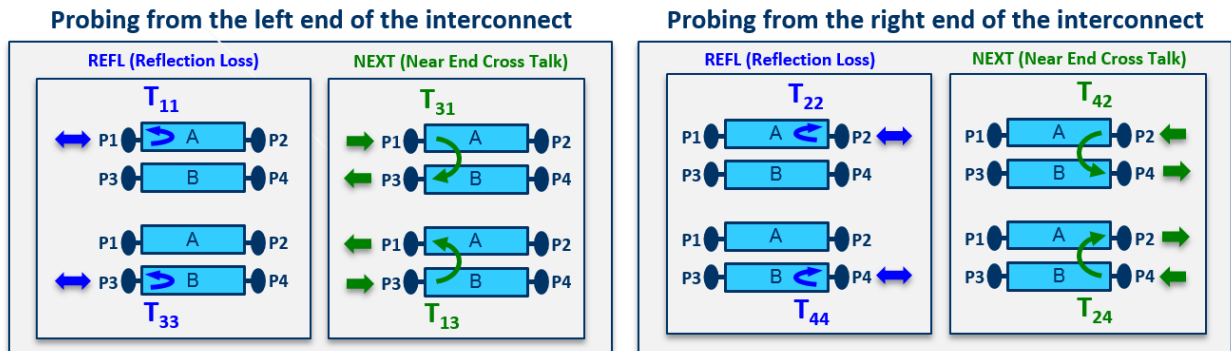
<sup>1</sup> For a detailed discussion of the REFL ratio, see the white paper, “Two Domains. Four Kinds of Ratios”.

<sup>2</sup> Laboratory grade TDR instruments often have multiple TDR heads, in which case, the two TDR heads can be connected to both P1 and P2 ports, and both T-parameter ratios can be measured simultaneously.

<sup>3</sup> A multi-head TDR can also be configured as a two-trace differential TDR, in which case the TDR source impedance will be 100 ohms instead of 50 ohms.

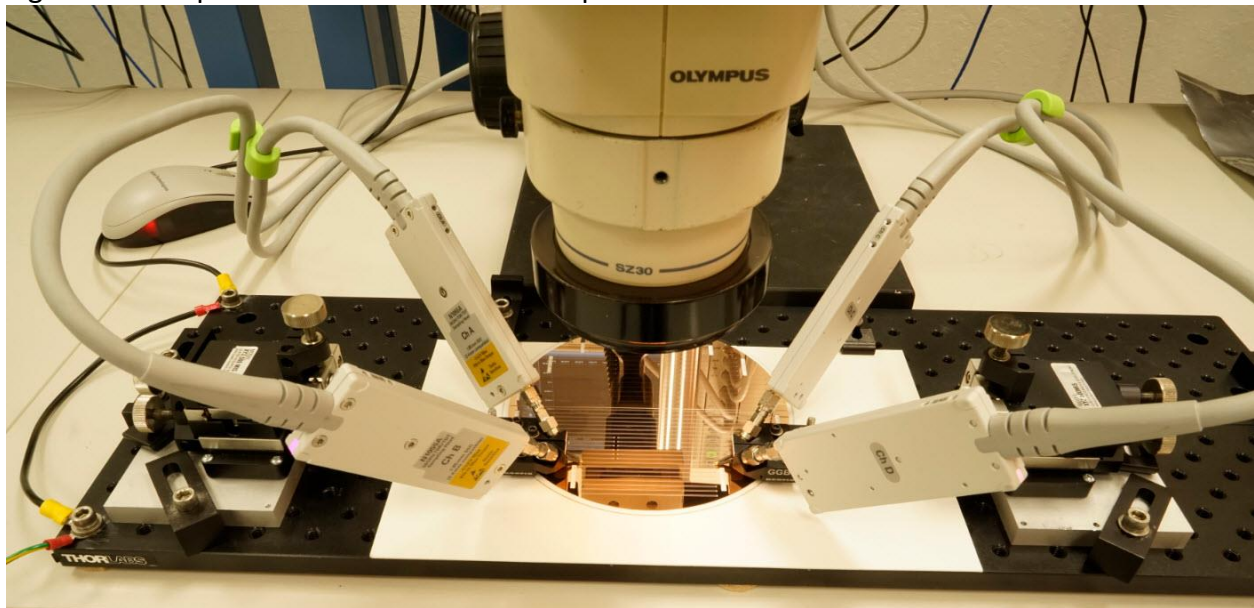
Coupled differential pair interconnects have four ports as shown in Figure 2. Because the two traces in the differential pair are coupled, part of the energy in the pulse that is injected into port P1 couples onto the other trace and exits the differential pair at port P3. In an analogous fashion, a portion of the energy in a pulse injected into port P2 will appear on port P4. One can also form a similar output/input ratio from these two coupling mechanisms, calling them NEXT (Near End Cross Talk), and using the same notational format introduced in previous paragraphs, designate them as  $T_{31}$  and  $T_{42}$  respectively. A similar set of REFL ratios can be defined for pulses injected into ports P3 and P4 respectively.

Figure 2: Parameters Needed to Compute Differential Pair Impedance



As with the single ended case, it is possible to connect a 4-head TDR to all 4 ports of a differential pair interconnects, in which case all 4 REFL and 4 NEXT T-parameter ratios can be measured simultaneously. An example of such a configuration is shown in Figure 2.

Figure 2: Example of a 4-Head TDR Test Setup



The impedance “looking” into each port can be calculated using equation (1). However, the differential impedance looking into Ports 1 and 3 simultaneously is not the simple sum of the

impedances looking into ports P1 and P3 using equation (1). The NEXT terms must first be subtracted from the REFL terms per the following equations:

$$\text{Left } TDD_{11} = \frac{1}{2} \cdot [(T_{11} - T_{13}) + (T_{33} - T_{31})] \quad \text{Left } Z_{\text{Diff}} = 100 \cdot \frac{1 + TDD_{11}}{1 - TDD_{11}} \quad (2a)$$

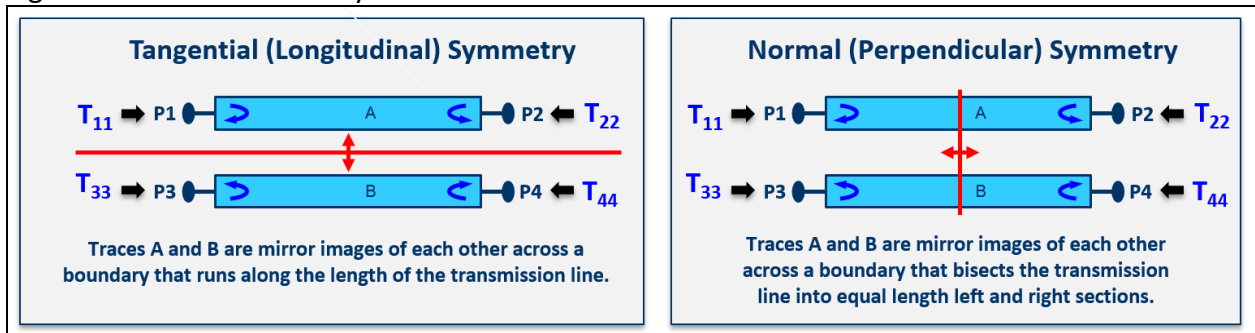
$$\text{Right } TDD_{11} = \frac{1}{2} \cdot [(T_{22} - T_{24}) + (T_{44} - T_{42})] \quad \text{Right } Z_{\text{Diff}} = 100 \cdot \frac{1 + TDD_{22}}{1 - TDD_{22}} \quad (2b)$$

If the diff pair traces are positioned close to each other, they are tightly coupled, and the NEXT ratios will have a relatively high numerical magnitude. If the differential pair traces are loosely coupled, then the NEXT ratios will have a relatively small numerical magnitude. As the two traces are moved closer together, the NEXT terms,  $T_{13}$ ,  $T_{31}$ ,  $T_{24}$  and  $T_{42}$ , increase in magnitude, and as a result, the corresponding REFL terms,  $T_{11}$ ,  $T_{22}$ ,  $T_{33}$  and  $T_{44}$ , must also increase (become more positive) if the desired differential impedance is to remain the same. An increase in the REFL ratios means the individual impedances of the traces must increase. One way to increase the REFL ratios is to decrease the trace width. However, this results in increased losses. This is why tightly coupled differential pair interconnects often have higher losses than loosely coupled differential pair interconnects. One way to get around this problem is to lower the differential impedance, for example, from 100 ohms to 85 ohms.

If there is no coupling between the two traces,  $T_{13} = T_{31} = T_{24} = T_{42} = 0$ , in which case the differential impedance is only dependent on the sum of the two REFL ratios,  $T_{11} + T_{33}$  or  $T_{22} + T_{44}$  respectively. Additional material on the NEXT ratios will be presented later on in this white paper.

In practical designs, the two traces in a differential pair are constructed to be physically identical. This can be expressed as the two symmetries as shown in Figure 2.

Figure 3: Differential Pair Symmetries



Referring to the left panel in Figure 3, if the two traces are mirror images of each other about the tangential (longitudinal) axis of the interconnect, then

$$T_{11} = T_{33} \quad T_{22} = T_{44} \quad (3)$$

Referring to the right panel in Figure 3, if the left half of the interconnect and the right half of the interconnect are mirror images of each other they have normal (perpendicular) symmetry, and

$$T_{11} = T_{22} \quad T_{33} = T_{44} \quad (4)$$

If an interconnect exhibits both symmetries, then

$$T_{11} = T_{22} = T_{33} = T_{44} \quad (5)$$

These symmetries can be used to quantify the “quality” of the differential pair interconnect – assuming the two traces in the differential pair are identical. Figures 3 and 4 graphically show the four REFL T-parameters for two coupled differential pair interconnects, “A” and “B” using equation 1.

Referring to the right graphs in Figures 4 and 5, one can see that the magnitude of the tangential symmetry (trace A – trace B) is smaller than the normal symmetry (left half of the interconnect minus the right half of the interconnect). This is almost always the case for coupled differential pair interconnects.

Figure 4: Differential Pair “A” Symmetries

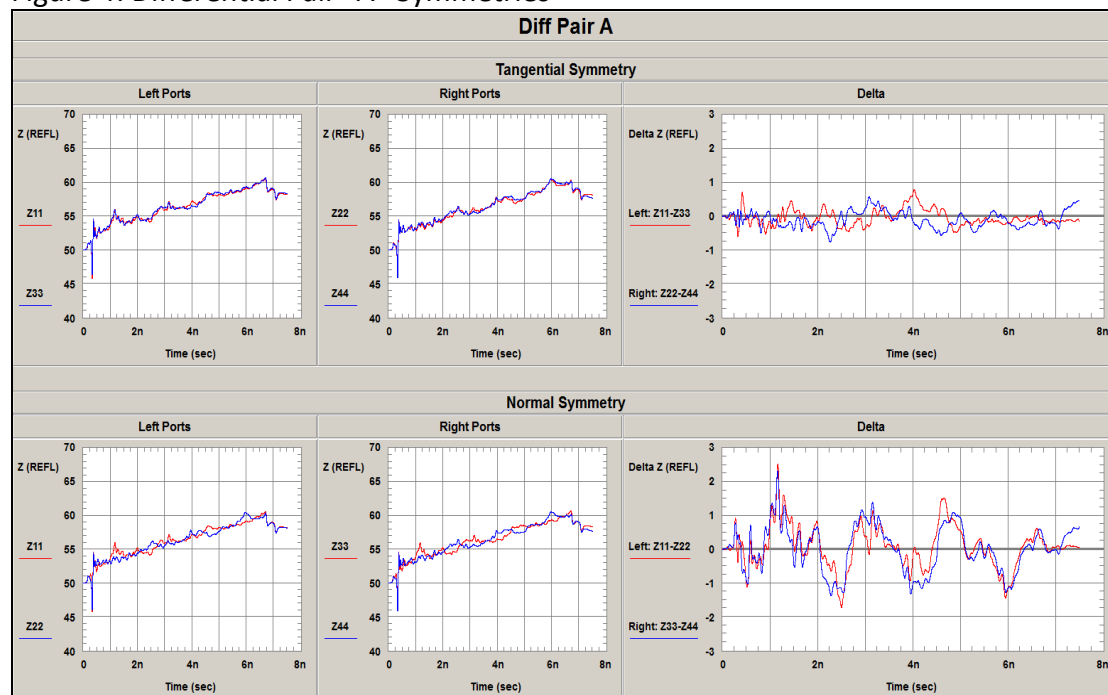
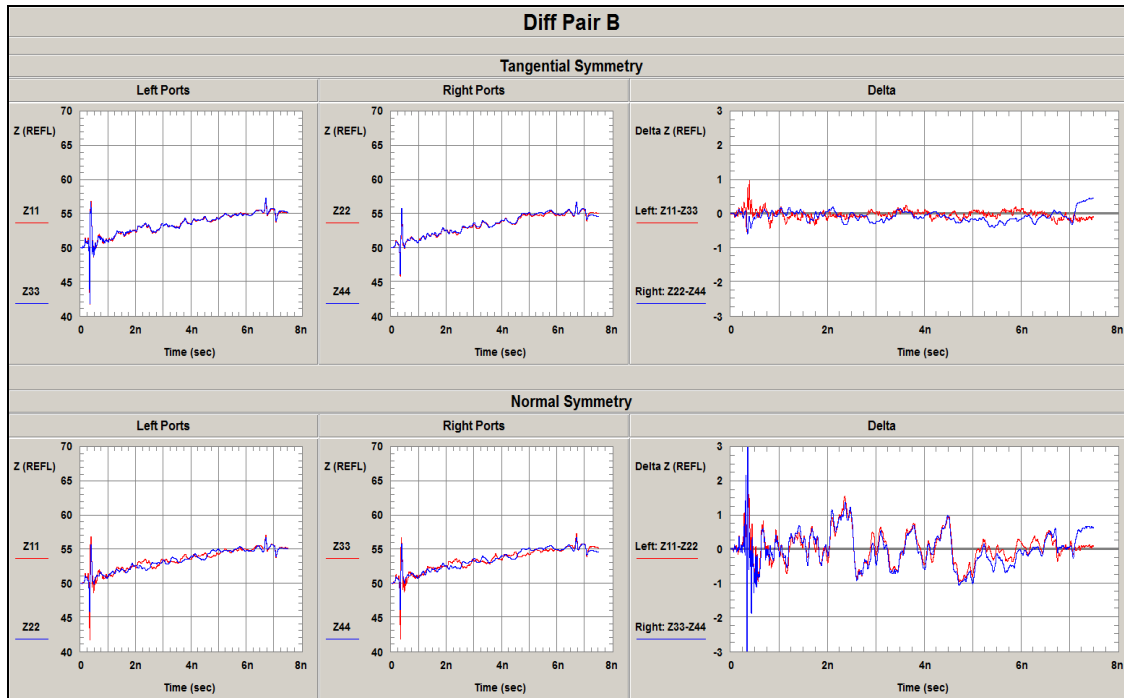


Figure 5: Differential Pair “B” Symmetries

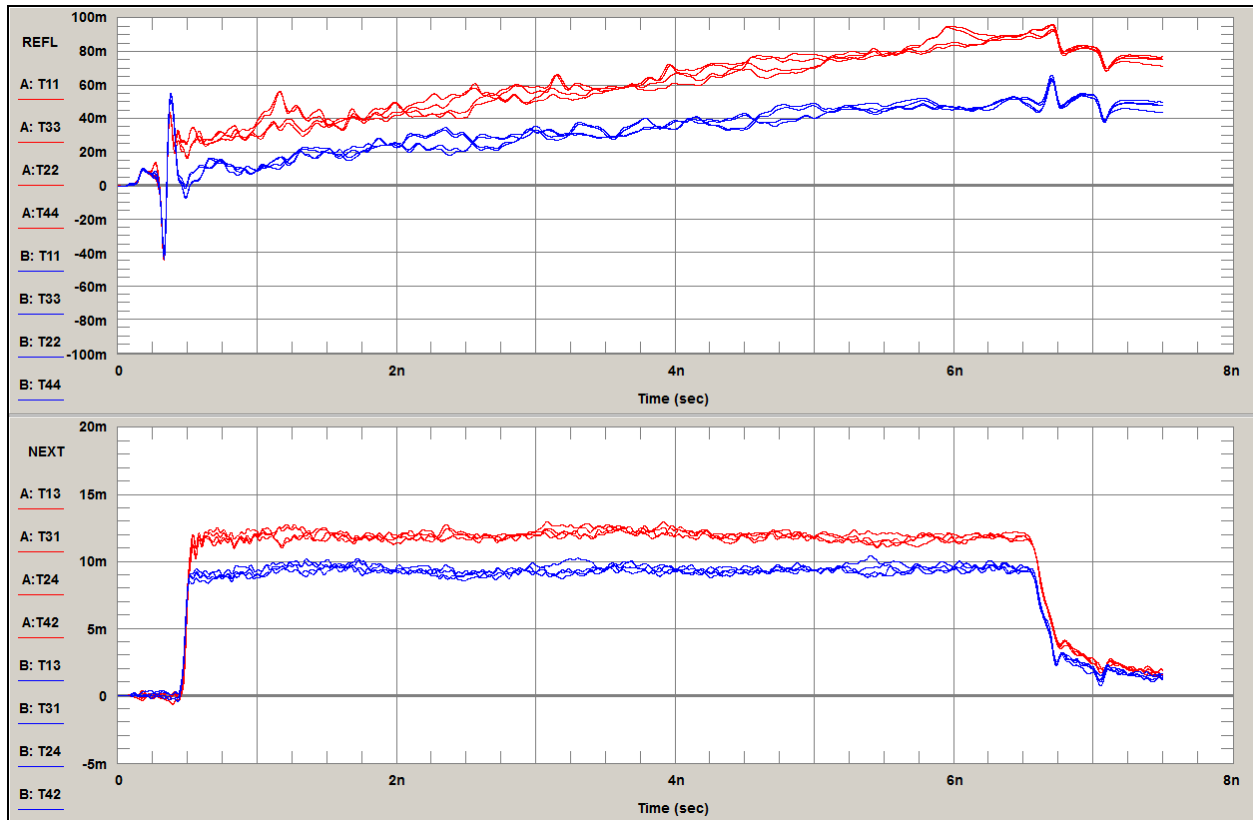


The anisotropic properties of the dielectrics used in the construction of the differential pair interconnect often show up in the tangential delta data. For example, traces routed parallel to the warp and fill directions of a coarse glass weave structure will introduce sine-wave shaped periodicities. Variations across a panel often show up in the normal delta data.

### NEXT Ratios in Greater Detail

Referring back to equations (2a) and (2b), the coupled NEXT ratios,  $T_{13}$ ,  $T_{31}$ ,  $T_{24}$  and  $T_{42}$  subtract from the REFL ratios,  $T_{11}$ ,  $T_{33}$ ,  $T_{22}$  and  $T_{44}$ . For a tightly coupled differential pair, the magnitudes of these NEXT ratios are larger than for a loosely coupled differential pair. This in turn requires larger REFL ratios, which in turn requires higher trace characteristic impedances.

Figure 6: Impact of NEXT on REFL and Individual Trace Impedances



Referring to Figure 6, one can immediately see that differential pair B (red trace) is more tightly coupled than differential pair A (blue traces) because the REFL ratios are higher (more positive) and the NEXT ratios are higher.<sup>4</sup>

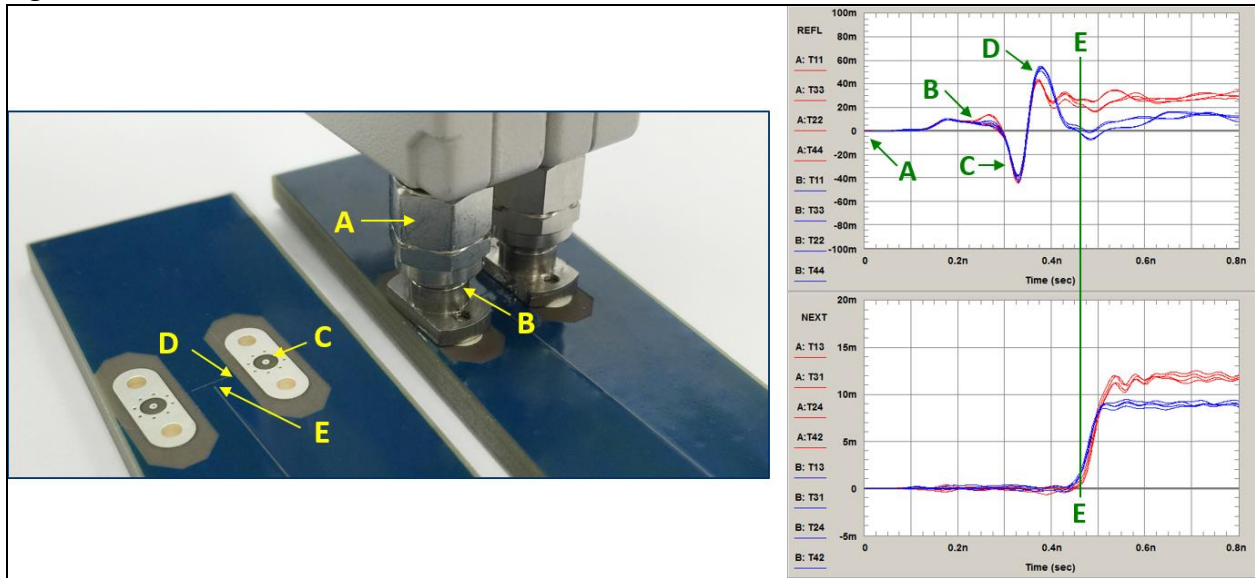
Figure 7 shows in greater detail the beginning of the curves in Figure 6, along with the launch structure. The references in Figure 7 correspond to the following physical structures:

- A: TDR calibration plane.
- B: Coaxial connector barrel – which has a slightly higher than 50 ohm impedance.
- C: Via structure – which has a significantly lower impedance (REFL ratio is a large negative value).
- D: Single ended trace connecting the via to the coupled differential pair transmission line. Note that the impedance is also greater than 50 ohms. This is often the case when the width of these single ended traces are kept at the same width of the trace when it reaches the differential pair.
- E: Beginning of the coupled differential pair transmission line.

As expected, the NEXT coupling ratios remain close to zero before the coupled transmission line, starting at location E, because the two traces are physically too far apart for significant coupling to take place.

<sup>4</sup> A detailed discussion of why the NEXT curve is horizontal is given in reference [9].

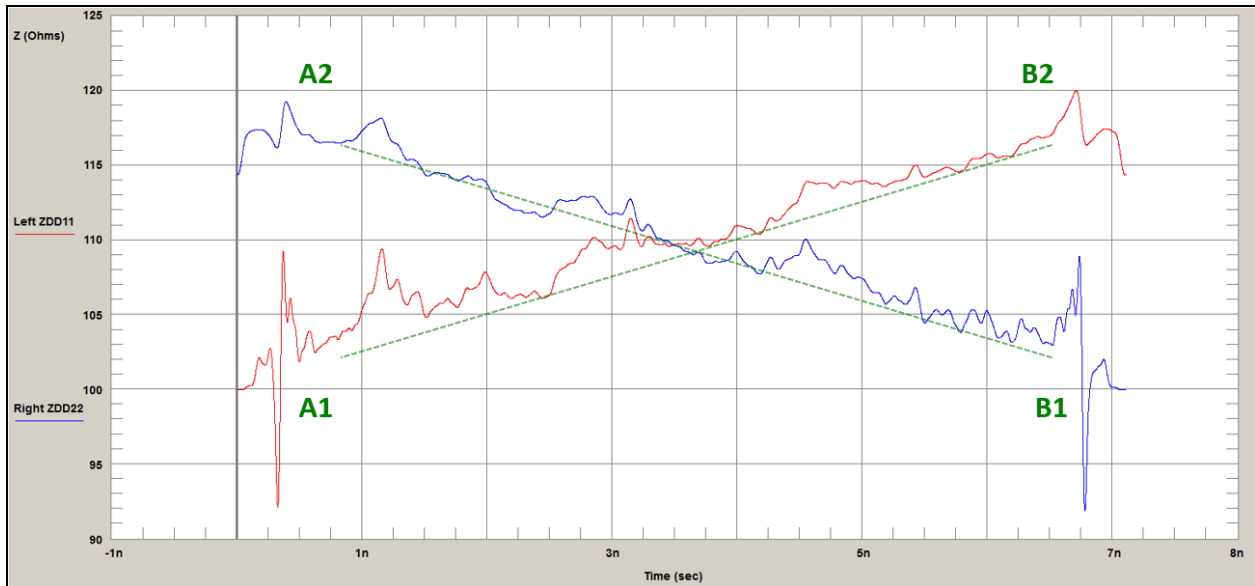
Figure 7: NEXT/REFL Launch Detail



### Impact of Interconnect Losses on Measured Impedance

Figure 8 is a plot of the differential impedances of lossy interconnect “A” as measured from the left (red curve,  $ZDD_{11}$ ) and right (blue curve,  $ZDD_{22}$ ) ends as calculated using equations (2a) and (2b). The curve for  $ZDD_{22}$  is reversed so it anatomically coincides with the impedance the TDR measures when connected to the right end of the interconnect. Region A1 is the calculated impedance in the vicinity of the left P1 port as measured by the TDR head connected to the left P1 port. Region A2 is the calculated impedance in the vicinity of the left P1 port as measured by the TDR head connected to the right P2 port. Similarly, A2 and B2 are the calculated impedances in the vicinity of the right P2 port when measured with the TDR heads connected to ports P1 and P2 respectively.

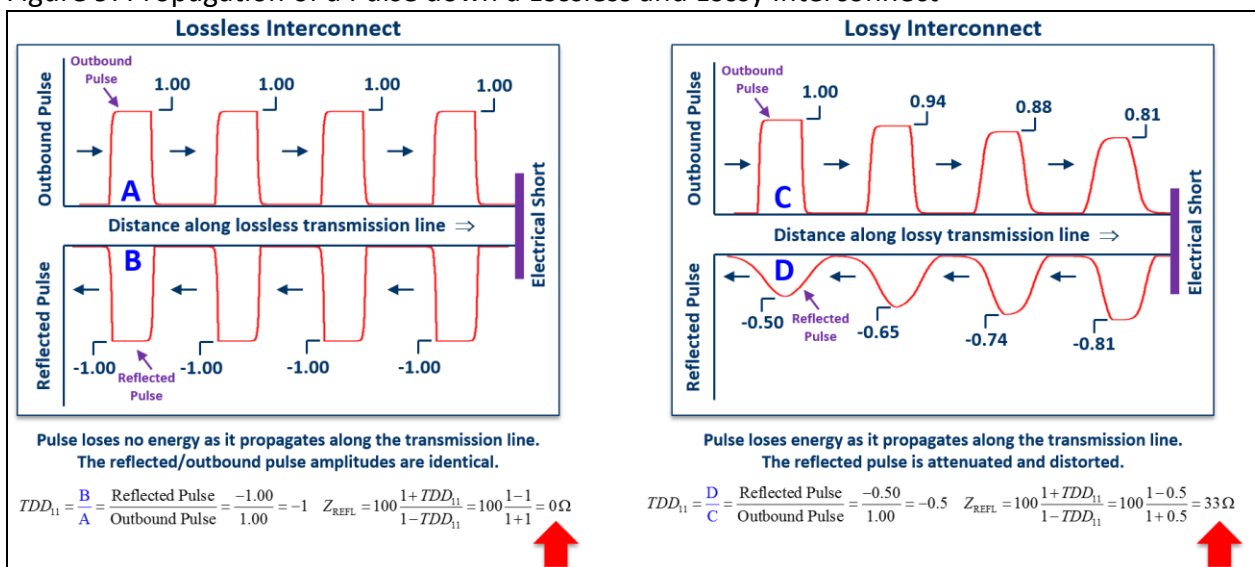
Figure 8: Differential Impedances for Interconnect “A”



Comparing the A1/A2 and B1/B2 impedances one can see that they differ by approximately 15 ohms. So which ones are correct? A1 and B1? Or A2 and B2? To answer these questions, one must look at what happens to the outbound pulse as it propagates down a lossy transmission line.

Referring to the left half of Figure 9, a pulse propagating down a lossless interconnect retains its shape and amplitude. If this pulse encounters a short at the end of the interconnect, it will reflect back with an opposite polarity, but keep its amplitude and shape intact. Calculating the impedance using equation (2), one arrives at an impedance of 0 ohms for the short at the end of the interconnect.

Figure 9: Propagation of a Pulse down a Lossless and Lossy Interconnect



However, if the interconnect is lossy, the pulse amplitude will decrease and its shape will distort (flatten out) as it propagates down towards the short and back towards the port the TDR is connected to. Calculating the impedance of the short at the end of the interconnect, again using equation (2), the impedance of the short at the end of the interconnect is now computed to be 33 ohms, significantly higher than the 0 ohms measured when a lossless interconnect was attached to the short. This is the reason why, in Figure 8, the impedances near the left end of the interconnect when measured from the right end of the interconnect appear to be higher than when they are measured from the closer left end. Ditto for B1 and B2.

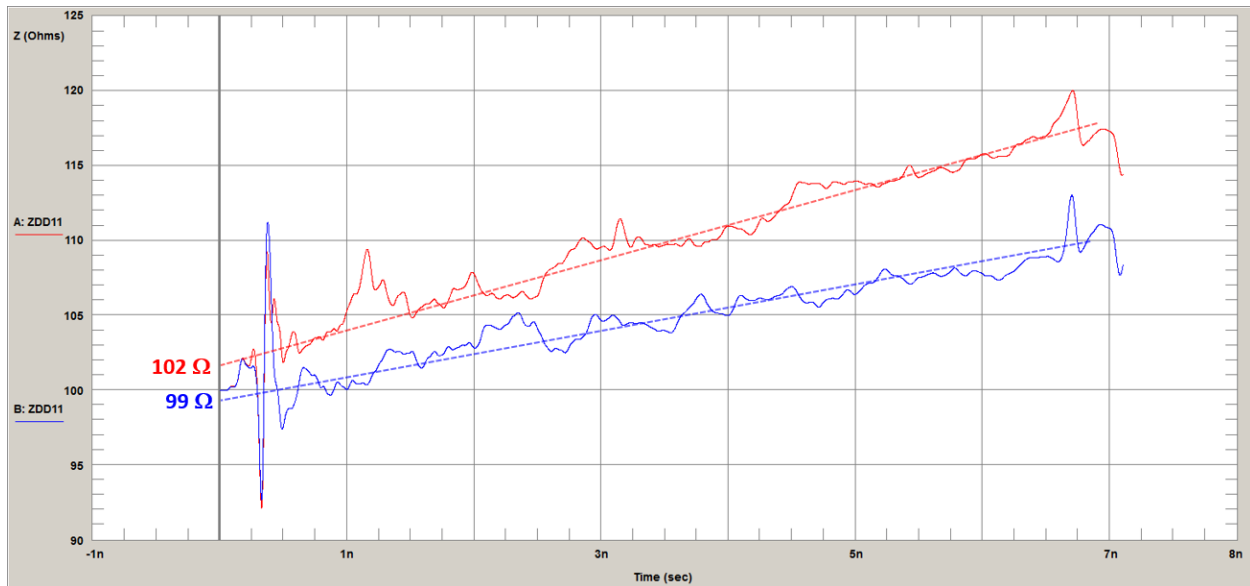
From this example, one can deduce that lossy interconnects raise the apparent impedance of the interconnect the farther into the interconnect the TDR pulse is allowed to propagate. One practical outcome of this phenomena is that long lossy interconnects need to be measured from both ends, not just one end.

The losses also have an impact on the spatial resolution. Comparing A1 with A2 and B1 with B2 in Figure 8, one can readily see that the spatial resolution decreases as the pulse propagates down a lossy interconnect. This problem is exasperated because the pulse has to propagate down the interconnect twice – once towards the structure where the impedances are not constant, and again all the way back.

### **The Importance of Slope in Characterizing Lossy Interconnects**

Figure 10 compares the calculated impedances of the more lossy tightly-coupled differential pair “A” (the red curve) and the less lossy loosely-coupled differential pair “B” (blue curve). Notice that in both cases, the impedances near the left end are well within the +/- 10% tolerance for a nominal 100 ohm characteristic impedance-based interconnect. Near the right end, however, the lossy “A” interconnect now appears to exceed the + 10% tolerance, while the less lossy “B” interconnect appears to approach dangerously close to the + 10% tolerance limit.

Figure 9: The Importance of Slope in Characterizing Lossy Interconnects



One potential way to circumvent this “rising slope” problem, is to extrapolate the logic presented in the previous section and make the claim that the impedance at the left end of these two rising sloped waveforms are more accurate indicators of the characteristic impedance of the interconnect than the right end.

This approach, however, ignores the losses associated with the interconnect. Again, referring back to Figure 9, the slope of the rising impedance curves is loss dependent. The higher the losses, the steeper the slope. Ignoring the slope by only concentrating on the left end of the impedance waveforms is analogous to “sweeping losses under the rug”, something that the author of this white paper does not believe is a proper approach to characterizing lossy interconnects using a TDR.<sup>5</sup>

This rising slope poses a problem as long as commercial TDR instruments used in a manufacturing environment continue to only offer horizontal limit lines, as opposed to sloping limit lines. For example, the use of horizontal limit lines often forces the PCB manufacturer to lower the characteristic impedance of the interconnect so the entire sloping TDR curve fits inside the horizontal limit lines. This has the effect of artificially tightening the impedance tolerances.

## Conclusions

The T-parameter ratio measurements from a TDR instrument can be used to calculate the impedance “looking” into one or both ends of single ended and differential pair interconnects.

<sup>5</sup> There is a commercially available software package that does exactly this – use a linear curve fit of a rising impedance curve to extrapolate a lossless impedance from a lossy interconnect.

If the losses are small, then the impedance as a function of time will be relatively constant, and hence it is numerically equivalent to the characteristic impedance of the interconnect.

However, if the losses are large, then the impedance curve will have a rising slope whose magnitude is proportional to losses in the interconnect.

### **About the Author:**

Franz Gisin is Director of Signal Integrity at Multek's Interconnect Technology Center in Milpitas, California. Franz Gisin's core focus is the electrical characterization of PCB-based high performance digital, RF and microwave interconnects.

Prior to Multek, Franz Gisin has worked for over 40 years in electromagnetics including EMC (Electromagnetic Compatibility), signal integrity and the characterization and modeling of high performance interconnects.

Franz Gisin has a BS in Electrical Engineering and an MS in Applied Mathematics.

### **About Multek's Interconnect Technology Center (ITC):**

The Interconnect Technology Center (ITC) is Multek's advanced technology development organization. We engage with customers early in the design process to create innovative solutions to pressing technical challenges. Our technical core competencies are aligned to meet the challenges of trends around increasing data rates, increasing density of PCBs, and new shape requirements.



TDR Measurements of PCB Interconnect Artifacts  
March 2017

Author: Franz Gisin

Multek  
17<sup>th</sup> Floor, Nina Tower (Tower II)  
8 Yeung Uk Road, Tsuen Wan  
New Territories, Hong Kong

Worldwide Inquiries:  
Phone: +852 2276 1800  
Fax: +852 2276 1434  
multek.com

### **References**

- [1] Ping Liu; Jingping Zhang; Jiayuan Fang, "Accurate characterization of lossy interconnects from TDR waveforms," *Electrical Performance of Electronic Packaging and Systems (EPEPS)*, 2013 IEEE 22nd Conference on, pp.187,190, 27-30 Oct. 2013.
- [2] Jaehoon Jeong; Nevels, R., "Novel time domain analysis technique for lossy nonuniform transmission lines," *Antennas and Propagation Society International Symposium*, 2005 IEEE, vol.3A, no., pp.848,851 vol. 3A, 3-8 July 2005.
- [3] Komuro, T., "Time-domain analysis of lossy transmission lines with arbitrary terminal networks," *Circuits and Systems, IEEE Transactions on*, vol.38, no.10, pp.1160, 1164, Oct 1991.
- [4] Heydari, P.; Abbaspour, S.; Pedram, M., "A comprehensive study of energy dissipation in lossy transmission lines driven by CMOS inverters," *Custom Integrated Circuits Conference, 2002. Proceedings of the IEEE 2002*, pp.517,520, 2002.
- [5] Brian C. Wadell, *Transmission Line Design Handbook*, Artech House, Inc., 1991.
- [6] Lawrence N. Dworsky, *Modern Transmission Line Theory and Applications*, Wiley-Interscience, 1979.
- [7] Richard E. Matlick, *Transmission Lines for Digital and Communication Networks*, McGraw-Hill, 1969.
- [8] Fred E. Gardiol, *Lossy Transmission Lines*, Artech House, 1987.
- [9] C.W. Davidson, *Transmission Lines for Communications*, Halsted Press, 1978.

Copyright © 2017, Multek and/or its affiliates. All rights reserved. This document is provided for information purposes only and the contents hereof are subject to change without notice. This document is not warranted to be error-free, nor subject to any other warranties or conditions, whether expressed orally or implied in law, including implied warranties and conditions of merchantability or fitness for a particular purpose. We specifically disclaim any liability with respect to this document and no contractual obligations are formed either directly or indirectly by this document. This document may not be reproduced or transmitted in any form or by any means, electronic or mechanical, for any purpose, without our prior written permission.

Multek is a registered trademark of Multek and/or its affiliates. Other names may be trademarks of their respective owners.